Inductance and resistance calculations for isolated conductors

K.F. Goddard, A.A. Roy and J.K. Sykulski

Abstract: Various analytical and numerical calculation methods for computing the high-frequency and low-frequency inductance and resistance of isolated conductors are reviewed. The high-frequency estimates are obtained using conformal mapping theory. In both cases, a uniformly distributed return current at an arbitrary radius is assumed. Formulae are presented for the inductance of a strip conductor of zero thickness. The inductance is computed both for DC and for AC infinite conductivity. For regular polygons the conformal mapping is defined by a power series, whereas finite element analysis is used to compute the DC inductance. Conformal mapping theory is used to obtain estimates of the resistance and inductance of a rectangular conductor when the skin depth is small compared to the thickness of the conductor. A method is then presented for calculating the resistance when the skin depth exceeds the thickness of the conductor but remains small in relation to the width of the conductor. Finite element analysis is used to confirm that one of the two resistance estimates always gives a reasonable estimate of the resistance.

1 Use of conformal mappings

For a conductor that has a remote return path, the return current has little effect on the field near the conductor. It may then be appropriate to calculate the flux linkage driven by the two currents separately. If the return current is uniformly distributed around a circle of radius R_{return} that completely encloses the conductor, the field of the return current lies completely outside this circle and therefore contributes nothing to the inductance. If the conductors can be considered infinitely conducting, i.e. the flux penetrating the conductors may be neglected, we only have to model the space outside the conductors. In this space, the potential satisfies the Laplace equation; hence, a conformal mapping may be used. A conformal transformation is a mapping defined by an analytic function $f(u) = z$ which maps complex u-space for which a solution is known to complex z-space which represents the real geometry of the problem. To obtain the distribution of potential using a conformal mapping, we require a mapping that will transform a simpler set of boundaries for which the solution is known to the real boundaries of the space to be modelled.

For an isolated conductor it is convenient to map the unit circle on to the surface of the conductor. The scalar magnetic potential and vector potential for the unit circle are given by

$$\Omega = \frac{\theta I}{2\pi} \quad \text{and} \quad A = \frac{\mu_0 I}{2\pi} \ln r$$

where r and θ are defined by $u = r\exp(j\theta)$. Hence, we can define a complex potential:

$$\Psi = A + \mu_0 \Omega j = \frac{\mu_0 I}{2\pi} \ln u$$

IEE Proceedings online no. 20051057

doi:10.1049/ip-smt:20051057

Paper first received 25th March 2004. Originally published online: 25th November 2004

The authors are with the School of Electronics and Computer Science, University of Southampton, Southampton, UK

E-mail: J.K.Sykulski@soton.ac.uk

2 DC inductance of an infinitely thin strip

We may define the DC effective radius R_{eff} of an isolated conductor such that the inductance of the conductor is the same as that of a cylindrical conductor of radius R_{eff}:

$$\ln(R_{\text{eff}}) - \frac{1}{4} = \iint \frac{J_z}{I} \iint \frac{J_z}{I} \times \frac{1}{2} \ln((x-u)^2 + (y-v)^2)\, dx\, dy\, du\, dv \tag{1}$$

where the double integrals are taken over the area representing the cross-section of the conductor. The one-quarter term on the left-hand side represents the internal self-inductance of a straight cylindrical wire: see [1].

In the particular case of an infinitely thin strip of width $2a$ we have:

$$\ln(R_{\text{eff}}) - \frac{1}{4} = \int_{-a}^{a} \frac{1}{2a} \int_{-a}^{a} \frac{1}{2a} \ln|x-u|\, dx\, du = \ln(2a) - 3/2$$

Hence, $R_{\text{eff}} = 2\exp(-5/4)a \approx 0.573a$.

3 Inductance of an infinitely conducting infinitely thin strip

For the case of an infinitely thin strip of width 4, the conformal mapping $z: \mathbb{C} \to \mathbb{C}$ is given by:

$$z = u + \frac{1}{u}$$

Notice that the unit circle is mapped to the subset of the real axis that represents the surface of the conductor. If $u = \exp(t + j\theta)$ the circular flux lines in u-space are defined by constant values of t and are mapped to ellipses in z-space. The flux lines are represented by the solid curves in Fig. 1, whereas the dotted curves represent lines of constant scalar magnetic potential. The two sets of curves are parameterised by:

$$x = 2\cos\theta \cosh t$$

$$y = 2\sin\theta \sinh t$$

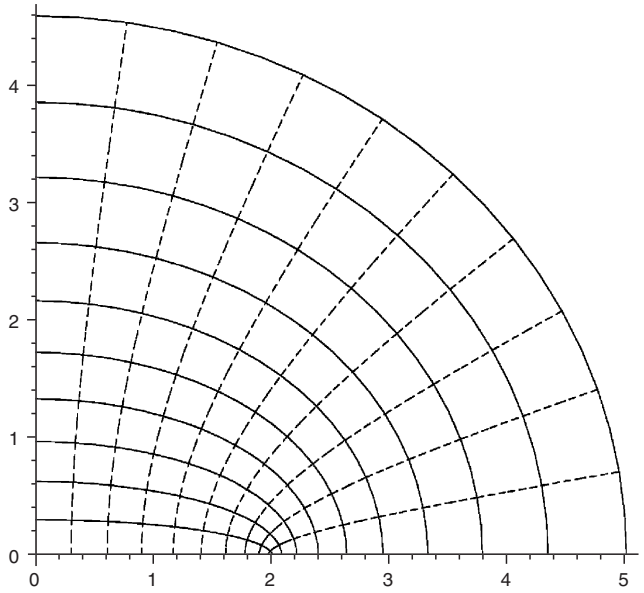

Fig. 1 *Contours of vector potential (solid) and scalar magnetic potential (dashed). Mirror symmetry exists along the real and imaginary axes*

The physical meaning of θ and t are defined by:

$$\theta = \frac{2\pi\Omega}{I} \quad \text{and} \quad t = \frac{2\pi}{\mu_0}\frac{A_z}{I}$$

where Ω and A_z represent the scalar and vector potential. In general, if the strip has a width of $2a$, the conformal mapping is given by:

$$z = R_{\text{eff}}\left(u + \frac{1}{u}\right)$$

where $R_{\text{eff}} = a/2$. Notice that when $|u|$ is large, $z \approx uR_{\text{eff}}$. This means that the inductance of the circuit is given by:

$$L = \frac{\mu_0}{2\pi}\ln\left(\frac{R_{\text{return}}}{R_{\text{eff}}}\right)$$

It is also possible to compute the surface $\boldsymbol{H}$ field on the strip:

$$H_x = \frac{d\Omega}{dx} = \frac{I}{2\pi}\left(\frac{d\theta}{dx}\right) = \frac{I}{2\pi\sqrt{a^2 - x^2}}$$

Notice the singularities which occur at $x = \pm a$. Despite the concentration of current at these singularities, the $\boldsymbol{H}$ field at $x = 0$ is still $(2/\pi)$ times its average value.

4 Regular polygons

In general, the conformal mapping which maps the unit circle on to a polygon can be derived from the Christoffel-Swartz transformation [2] and is given by:

$$z = F(u) = A\int \frac{(u-u_1)^{\beta_1}(u-u_2)^{\beta_2}\ldots(u-u_n)^{\beta_n}}{u^2}du \quad (2)$$

where $\pi\beta_k$ is the change in angle at the kth vertex of the polygon and $u_k = \exp(j\alpha_k)$. The values of α_k must be chosen to ensure the correct ratio of side lengths and A determines the overall size and orientation of the polygon. For a regular n-sided polygon, the values of u_k are uniformly distributed around the unit circle. The mapping is then given by:

$$z = F(u) = R_{\text{eff}}\int\left(1 - \frac{1}{u^n}\right)^{2/n}du$$

When $n \geq 2$, the indefinite integral cannot be expressed in terms of elementary functions. To overcome this difficulty a series expansion may be employed. From the binomial theorem:

$$\left(1 - \frac{1}{u^n}\right)^{2/n} = 1 + \frac{2}{n}\left(\frac{-1}{u^n}\right) + \frac{2(2-n)}{2!n^2}\left(\frac{-1}{u^n}\right)^2 + \ldots \quad (3)$$

Choosing a suitably large number of terms in the expansion and integrating term-by-term, an approximate expression for $F(u)$ may be obtained. For a square of effective radius of unity:

$$z = u + \frac{1}{6u^3} + \frac{1}{56u^7} + \frac{1}{176u^{11}} + \frac{1}{384u^{15}} + O\left(\frac{1}{u^{19}}\right)$$

Circles in complex u-space are mapped to the solid curves in Fig. 2.

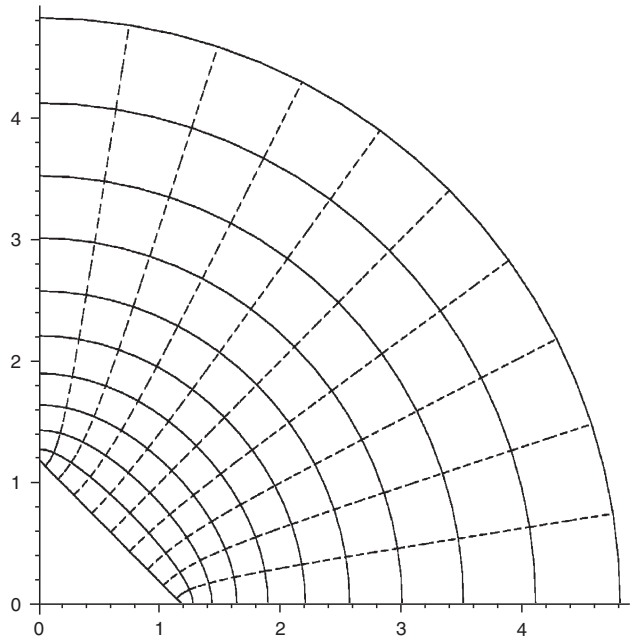

Fig. 2 *Contours of vector (solid) and scalar (dashed) potential when n = 4*

All that remains is to scale the result for the particular geometry in question. For a square of side length $2a$, the equivalent circular radius, R_{eff}, is given by:

$$R_{\text{eff}} = a\frac{\sqrt{2}}{z(1)} \approx 1.180\,35a \quad (4)$$

It is possible to express the integral:

$$F(u) = \int\sqrt{1 - \frac{1}{u^4}}du$$

in terms of elliptic functions. It can then be shown that:

$$\begin{aligned} R_{\text{eff}} &= a/\left|F(e^{i\pi/4})\right| \\ &= a\left|\text{elliptic}F\left(\frac{1}{\sqrt{2}} - \frac{i}{\sqrt{2}}, i\right)(i-1)\right. \\ &\quad \left. + \text{elliptic}E\left(\frac{1}{\sqrt{2}} - \frac{i}{\sqrt{2}}, i\right)(1-i) + 1\right|/\sqrt{2} \end{aligned}$$

which agrees with the value of R_{eff} found from the series expansion.

A graph showing R_{eff}/a as a function of the number of sides of the polygon has been obtained from (3)

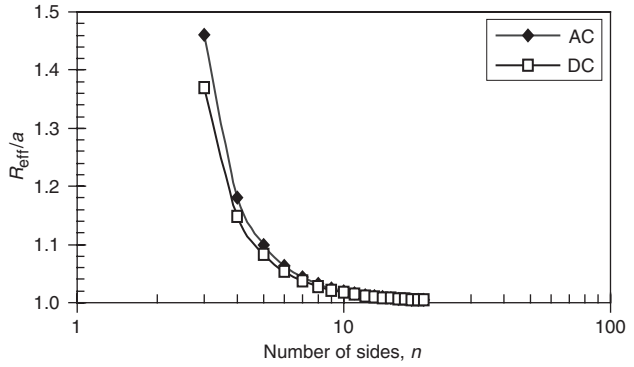

Fig. 3 *Graph showing the variation of R_{eff} with respect to n*

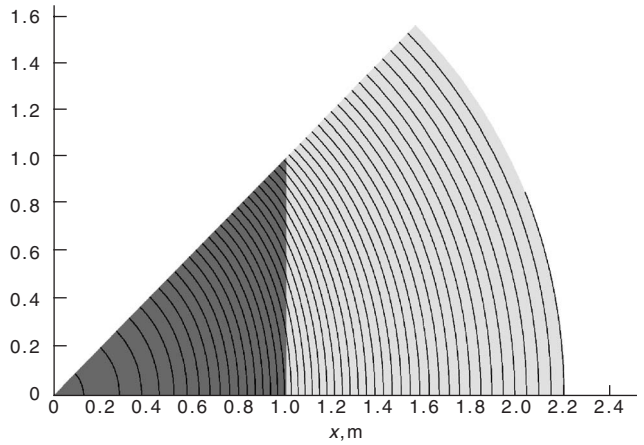

Fig. 4 *Finite element model showing contours of vector potential for the case of a four sided polygon, i.e. a square*

and is shown in Fig. 3. In this general case, a denotes the distance from the centre of the polygon to the midpoint of each side.

The DC equivalent radius for a series of polygons has been computed using finite element analysis and is also plotted in Fig. 3. A typical model is shown in Fig. 4. Due to symmetry, only a segment of the polygon has been modelled. The triangular region represents the conductor which carries a uniformly distributed current I. The return current $-I$ is represented by a boundary condition on the air region at radius R_{return}. If R_{return} is large it would be sufficient to impose a zero potential on this boundary. Alternatively, we could place the outer boundary closer to the conductor and impose a non-zero potential to represent the external field. The vector potential on the outer boundary is a function of θ. The vector potential in the air region is of the form:

$$A_z = \frac{\mu_0 I}{2\pi}\ln\left(\frac{R_{return}}{r}\right) + \sum_{k=1}^{\infty} A_k \cos(nk\theta) r^{-nk}$$

from which

$$B_r = -\sum_{k=1}^{\infty} nkA_k \sin(nk\theta) r^{-(nk+1)}$$

and

$$B_\theta = \frac{\mu_0 I}{2\pi r} + \sum_{k=1}^{\infty} nkA_k \cos(nk\theta) r^{-(nk+1)}$$

The model is first solved with a zero potential on the boundary; this will produce an increase in the value of B_θ and a corresponding reduction in the values of B_r. Hence, good approximations to the values of A_k are given by the average values of:

$$\frac{r^{nk+1}}{nk}(B_\theta \cos nk\theta - B_r \sin nk\theta)$$

around a circle of radius r which lies between the conductor and the outer boundary. These values of A_k are then imposed on the outer boundary to obtain a more accurate solution. If there are significant eddy currents in the conductor or if the conductor is made of permeable material, changing the boundary potential will affect the internal source distribution; hence, further iterations may be required. This technique allows an infinite boundary to be modelled at a greatly reduced radius and is more computationally efficient, reducing the number of elements in the model. The DC inductance is then obtained from:

$$L = \frac{\iint \boldsymbol{A}.\boldsymbol{J}dS}{I^2}$$

making some obvious adjustments to cope with the symmetry. The effective DC radius is then obtained from:

$$R_{eff} = R_{return}\exp\left(\frac{-2\pi L}{\mu_0} + \frac{1}{4}\right)$$

5 DC inductance of a rectangular conductor

The DC effective radius of an isolated rectangular strip can be found from (1). For a strip of width $2a$ and thickness $2b$, (1) becomes:

$$\ln(R_{eff}e^{-1/4}) = \frac{1}{16a^2b^2}\int_{-b}^{b}\int_{-a}^{a}\int_{-b}^{b}\int_{-a}^{a}\frac{1}{2}\ln((x-u)^2 + (y-v)^2)dx\,dy\,du\,dv$$

This integral evaluates to give:

$$\ln(R_{eff}e^{-1/4}) = \frac{1}{12a^2b^2} \times \left\{\begin{array}{l}(8a^3b - 8b^3a)\tan^{-1}(b/a) + (-a^4 + 6b^2a^2 - b^4)\ln(b^2 + a^2) \\ -25b^2a^2 + 4\pi ab^3 + 2b^4\ln(b) + 12a^2b^2\ln(2) + 2a^4\ln(a)\end{array}\right\}$$

6 Inductance of an infinitely conducting rectangular conductor

As discussed in Section 2, the field of a conductor of infinite conductivity may be obtained by the use of a conformal mapping. For the case of a rectangular conductor, the mapping from the unit circle is given by:

$$\begin{aligned} z &= F(u) \\ &= R_{eff}\int [(u-u_1)(u-u_2)(u-u_3)(u-u_4)]^{1/2}/u^2 du \end{aligned} \quad (5)$$

where $u_1 = e^{i\theta}$, $u_2 = e^{-i\theta}$, $u_3 = -e^{i\theta}$, $u_4 = -e^{-i\theta}$.

The value of θ is chosen to give the correct ratio of the two dimensions of the rectangle. If $2a$ and $2b$ are the dimensions of the rectangle, θ is found by solving the equation $bF(1) + aiF(i) = 0$. The radius R_{eff} of an equivalent cylindrical conductor can then be found such that $a = F(1)$. Figure 5 shows the variation in the effective radius both for DC and AC infinite conductivity as a function of the ratio of the sides of the rectangle.

The required expressions for $F(1)$ and $F(i)$ in terms of R_{eff} and θ may be found from (5) which simplifies to

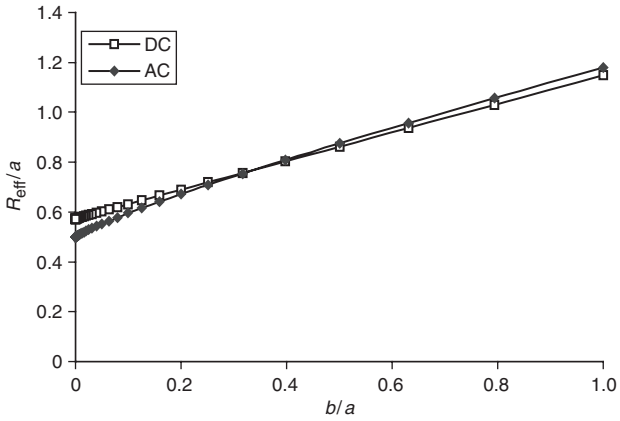

Fig. 5 *The effective radius as a function of b/a*

give:

$$z = F(u) = R_{\text{eff}} \int [1 + u^{-4} - 2u^{-2}\cos(2\theta)]^{1/2} du \qquad (6)$$

As for the other polygons, it is difficult to obtain the indefinite integral. An expression for $F'(u)$ may be obtained using a series expansion.

In general, from [3]:

$$(1 - 2xc + x^2)^{-1/2} = \sum_{n=0}^{\infty} P_n(c)x^n \qquad (7)$$

where $P_n(c)$ is the nth Legendre polynomial. By multiplying both sides of (7) by $(1-2xc+x^2)$ and comparing like terms in x we find that:

$$(1 - 2xc + x^2)^{1/2} = 1 - cx + \sum_{n=2}^{\infty} \beta_n x^n$$

where $\beta_n(c) = P_n(c) - 2cP_{n-1}(c) + P_{n-2}(c)$.

Setting $x = u^{-2}$, this result implies that:

$$F'(u) = R_{\text{eff}}\left(1 - \frac{c}{u^2} + \sum_{n=2}^{\infty} \beta_n(c)u^{-2n}\right)$$

where $c = \cos 2\theta$ and so

$$F(u) = z = R_{\text{eff}}\left(u + \frac{c}{u} + \sum_{n=2}^{\infty} \frac{\beta_n(c)}{(-2n+1)}u^{-2n+1}\right) \qquad (8)$$

the first few terms of which are

$$z = R_{\text{eff}}\left(u + \frac{\cos 2\theta}{u} - \frac{(1 - \cos^2 2\theta)/2}{3u^3} - \frac{(\cos 2\theta - \cos^3 2\theta)/2}{5u^5} + \cdots\right)$$

This function maps the unit circle on to the surface of the conductor. Circles whose radius exceeds unity are mapped on to the solid curves in Fig. 6.

7 High-frequency resistance of an isolated rectangular strip

When the frequency is infinite, the losses are also infinite since the current density is infinite on the surface of the conductor. In the case of a finite frequency when the skin depth Δ is small compared to the thickness of the conductor, the loss may be estimated using the surface $\boldsymbol{H}$ field for zero Δ. The losses are obtained from the integral of the Poynting vector around the surface of the conductor which gives the power flow into the

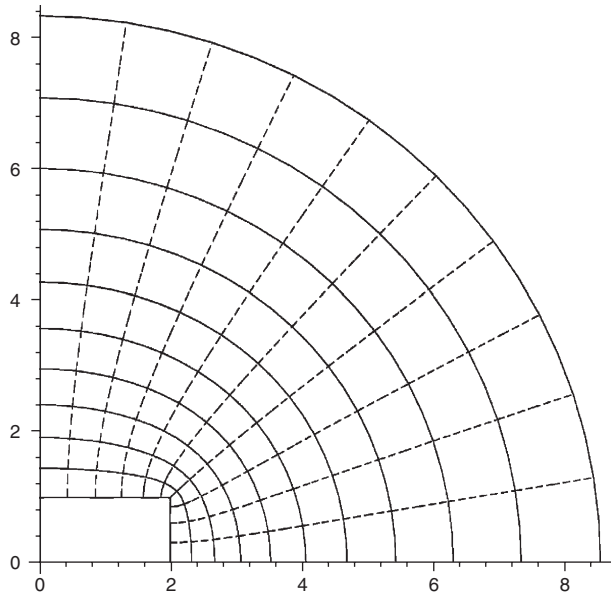

Fig. 6 *Contours of vector and scalar potential for a rectangular strip*

conductor, i.e.:

$$\text{power flow} = \oiint (\boldsymbol{E} \times \boldsymbol{H}) \cdot d\boldsymbol{S}$$

For the 2-D case considered:

$$H_z = 0 \quad \text{hence} \quad (\boldsymbol{E} \times \boldsymbol{H}).\hat{\boldsymbol{n}} = E_z H_{\text{surf}}$$

and

$$R = \frac{\int \left(\oint E_z H_{\text{surf}} ds\right) dt}{\int I^2 dt}$$

where the time integrals are taken over a full period of the current waveform. If the skin depth is small in relation to the dimension of the rectangle a reasonable approximation can be obtained by assuming that E_z and H_{surf} are related by a 1-D diffusion equation. If it is also assumed that the current waveform is sinusoidal, we find that

$$\frac{\int E_z H_{\text{surf}} dt}{\int H_{\text{surf}}^2 dt} = \frac{1}{\sigma\Delta}$$

and hence

$$R = \frac{1}{\sigma\Delta} \oint \frac{H_{\text{surf}}^2}{I^2} dl \qquad (9)$$

The integral $H_{\text{surf}}^2 \mathrm{d}l$ in z-space may be converted into an integral around the unit circle in u-space:

$$|H_{\text{surf}}| = \frac{I}{2\pi}\left|\frac{du}{dz}\right|_{|u=\exp(it)}$$

and

$$\oint H_{\text{surf}}^2 dl = \int_0^{2\pi} \left(\frac{I}{2\pi}\right)^2 \left|\frac{du}{dz}\right|_{|u=\exp(it)} dt$$

Hence (9) becomes:

$$R = \frac{1}{4\pi^2\Delta\sigma} \int_0^{2\pi} \left|\frac{du}{dz}\right|_{|u=\exp(it)} dt \qquad (10)$$

From (5):

$$\frac{dz}{du}_{|u=\exp(it)} = R_{\text{eff}}[(e^{it} - e^{i\theta})(e^{it} - e^{-i\theta})(e^{it} + e^{i\theta})(e^{it} + e^{-i\theta})]^{1/2}/e^{2it}$$

hence

$$\left|\frac{dz}{du}\right|_{|u=\exp(it)} = R_{\text{eff}}\left[16\sin\left(\frac{t-\theta}{2}\right)\sin\left(\frac{t+\theta}{2}\right)\times\sin\left(\frac{t-\pi-\theta}{2}\right)\sin\left(\frac{t-\pi+\theta}{2}\right)\right]^{1/2}$$

From (10), the resistance is given by the elliptic integral:

$$R = \frac{1}{4\pi^2 R_{\text{eff}}\sigma\Delta}\int_0^{2\pi}\frac{dt}{\sqrt{|2\cos 2\theta - 2\cos 2t|}} \quad (11)$$

Note that

$$\int_0^{2\pi}\frac{dt}{\sqrt{|2\cos 2\theta - 2\cos 2t|}} = 2\int_0^{\pi/2}\frac{dt}{\sqrt{|\cos^2\theta - \cos^2 t|}}$$
$$= 2\int_0^{\theta}\frac{dt}{\sqrt{\sin^2\theta - \sin^2 t}} + 2\int_\theta^{\pi/2}\frac{dt}{\sqrt{\cos^2\theta - \cos^2 t}}$$

Making the substitution $s = \cos(t)/\cos(\theta)$ the second integral becomes:

$$2\int_0^1\frac{ds}{\sqrt{1-s^2}\sqrt{1-s^2\cos^2\theta}}$$

and since elliptic$K(k)$ is defined to be:

$$\int_0^1\frac{dt}{\sqrt{1-t^2}\sqrt{1-k^2t^2}}$$

R is given by

$$R = \frac{1}{2\pi^2 R_{\text{eff}}\sigma\Delta}(\text{elliptic}K(\sin\theta) + \text{elliptic}K(\cos\theta)) \quad (12)$$

A method for evaluating elliptic$K(k)$, which is described in [3], is given as follows. We begin with the triplet of numbers:

$$l_0 = 1, \quad m_0 = \sqrt{1-k^2}, \quad n_0 = k$$

Successive iterations of l_i, m_i and n_i are found by taking:

$$l_i = \frac{1}{2}(l_{i-1} + m_{i-1}), \quad m_i = \sqrt{l_{i-1}m_{i-1}},$$
$$n_i = \frac{1}{2}(l_{i-1} - m_{i-1})$$

Convergence is achieved when p is such that $n_p \approx 0$ and elliptic$K(k) = \frac{\pi}{2l_p}$. Hence, the resistance can be computed numerically from (12).

Since we have relaxed the assumption that $\Delta = 0$, some flux flows within the conductor leading to increased inductance. This additional inductance is given, to first-order, by:

$$\Re\left(\frac{A}{H}\right)\frac{\int H_{\text{surf}}^2 dl}{I^2} = \frac{R}{\omega}$$

where ω is angular frequency of the current.

8 High-frequency resistance of an isolated thin rectangular strip

When $b/a \to 0$, $\theta \to 0$ and the integral in (12) for R becomes infinite. For small θ, an asymptotic limit may be obtained by expanding the elliptic functions in terms of θ:

$$2R\sigma\Delta R_{\text{eff}} = \left(\ln 4 + \frac{\pi}{2} - \ln\theta\right)/\pi^2 + O(\theta^2) \quad (13)$$

First-order approximations for a and b are given by:

$$a = 2R_{\text{eff}} + O(\theta^2)$$

and

$$b = 2R_{\text{eff}}\left(\frac{\pi}{4}\theta^2 + O(\theta^4)\right). \quad (14)$$

The latter is obtained from (8) as follows.

$$\frac{b}{R_{\text{eff}}} = \frac{|F(i)|}{R_{\text{eff}}} = \left(\frac{|F(i)|}{R_{\text{eff}}}\right)_{|\theta=0} + \theta\frac{\partial}{\partial\theta}\left(\frac{|F(i)|}{R_{\text{eff}}}\right)_{|\theta=0} + \frac{\theta^2}{2!}\frac{\partial^2}{\partial\theta^2}\left(\frac{|F(i)|}{R_{\text{eff}}}\right)_{|\theta=0} + \ldots$$

Since the Legendre polynomials satisfy $P_n(1) = 1$ for all $n = 0, 1, 2\ldots$ it is clear that $\beta_n(1) = 0$; hence, $F(i) = 0$ when $\theta = 0$. Also, since c is an even function of θ, $\partial F(i)/\partial\theta = 0$ at $\theta = 0$, and

$$\left(\frac{1}{R_{\text{eff}}}\frac{\partial^2|F(i)|}{\partial\theta^2}\right)_{|\theta=0} = \left(\frac{1}{R_{\text{eff}}}\frac{\partial|F(i)|}{\partial c}\frac{\partial^2 c}{\partial\theta^2}\right)_{|\theta=0} = \frac{-4}{R_{\text{eff}}}\left(\frac{\partial|F(i)|}{\partial c}\right)_{c=1}$$

Hence, we obtain:

$$\frac{b}{2R_{\text{eff}}} = \frac{-4}{2R_{\text{eff}}}\frac{\theta^2}{2!}\left(\frac{\partial|F(i)|}{\partial c}\right)_{|c=1} + O(\theta^4)$$

From (8):

$$\frac{1}{R_{\text{eff}}}\left(\frac{\partial F(i)}{\partial c}\right)_{|c=1} = i\left(-1 + \sum_{n=2}^{\infty}\frac{(-1)^n\beta_n'(c)}{-2n+1}\right)_{|c=1}$$

Since $P_n'(1) = n(n+1)/2$, $\beta_n'(1) = -1$. Hence:

$$\frac{1}{R_{\text{eff}}}\left(\frac{\partial F(i)}{\partial c}\right)_{|c=1} = -i\left(1 - \frac{1}{3} + \frac{1}{5} - \frac{1}{7} + \ldots\right) = -i\frac{\pi}{4}$$

Hence, (14) follows.

Combining (13) and (14) we obtain:

$$R\sigma\Delta a = \frac{\ln 4}{\pi^2} + \frac{1}{2\pi} - \frac{\ln(4/\pi)}{2\pi^2} - \frac{\ln(b/a)}{2\pi^2} + O(b/a) \quad (15)$$

The dimensionless graph in Fig. 7 may be used to estimate the resistance of any rectangular conductor for which $\Delta < b$. For small values of b/a, the asymptote described by (15) is a good approximation to the semi-analytical results obtained using (12).

9 Low-frequency resistance of an isolated rectangular strip

In this Section, we obtain an approximation to the resistance when both b/Δ and b/a are small. First, we

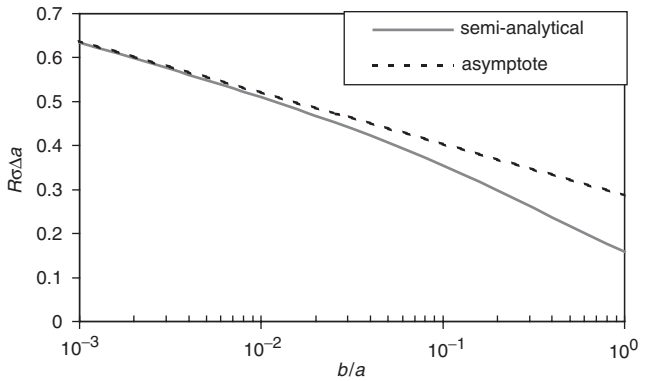

Fig. 7 *$R\sigma\Delta a$ plotted against the ratio b/a*

simplify the problem by neglecting the thickness, but not the thickness conductivity product, of the strip. This allows the simple mapping $z = a(u + 1/u)/2$ to transform the unit circle $u = \exp(i\tau)$ on to the surface of the strip of width $2a$ in complex z-space.

For an infinitely conducting strip, B_θ on the unit circle in u-space is given by,

$$B_\theta = \frac{\mu_0 I}{2\pi}$$

Hence, B_x on the top surface of the strip is given by:

$$B_x = \frac{-\mu_0 I}{2\pi a \sin\tau}$$

Since the real strip has a finite thickness conductivity product, flux can cut through the strip; hence, the conductor no longer represents a contour of vector potential. We therefore assume that A_z in complex u-space has the form:

$$-A_z = \frac{\mu_0 I}{2\pi}\ln(r) + A_0 + \sum_{k\ \text{even}} A_k r^{-k}\cos(k\tau)$$

where $A_0, A_2, A_4 \ldots$ are unknown complex coefficients.

Since $\boldsymbol{B} = \nabla \times \boldsymbol{A}$ we find that B_θ on the surface of the unit circle is given by:

$$B_\theta = \frac{\mu_0 I}{2\pi} - \sum_{k\ \text{even}} kA_k\cos(k\tau) \tag{16}$$

Also,

$$J = \sigma E = -\sigma\frac{dA}{dt} = j\omega\sigma(A_0 + \sum_{k\ \text{even}} A_k\cos(k\tau))$$

Since $H_x = -\int_0^b J dy$ we therefore deduce that B_x on the top surface of the rectangular strip is given by:

$$B_x = \mu_0 j\omega\sigma b(A_0 + \sum_{k\ \text{even}} A_k\cos(k\tau))$$

Since conformal transformations preserve $\int \boldsymbol{H}\cdot d\boldsymbol{l}$, B_θ in u-space is given by:

$$B_\theta = a|\sin\tau|\mu_0 j\omega\sigma b(A_0 + \sum_{k\ \text{even}} A_k\cos(k\tau)) \tag{17}$$

Equations (16) and (17) therefore imply that:

$$\frac{\mu_0 I}{2\pi} - \sum_{k\ \text{even}} kA_k\cos(k\tau) = \mu_0 j\omega\sigma ba|\sin\tau| \times (A_0 + \sum_{k\ \text{even}} A_k\cos(k\tau))$$

Now using

$$|\sin\tau| = \frac{2}{\pi}\left(1 - \sum_{k\ \text{even}}\frac{2\cos k\tau}{k^2 - 1}\right),$$

an infinite system of simultaneous equations may be constructed. We find that:

$$kA_k + CA_k + C\sum_{\substack{l=0\\ l\ \text{even}}}^{\infty}\left(\frac{1}{(k-l)^2 - 1} + \frac{1}{(k+l)^2 - 1}\right)A_l = 0$$

$k = 2, 4, 6 \ldots$

and

$$C\sum_{\substack{l=0\\ l\ \text{even}}}^{\infty}\frac{A_l}{l^2 - 1} = \frac{\mu_0 I}{2\pi} \quad k = 0$$

where $C = 2\mu_0 j\omega\sigma ba/\pi$.

By truncating the series, a finite set of linear simultaneous equations is obtained, which can be solved numerically to obtain the values of the unknown coefficients A_k.

The losses are obtained from the integral of the Poynting vector over the surface of the conductor, i.e.:

$$\text{losses} = \iint (\boldsymbol{E}\times\boldsymbol{H}).d\boldsymbol{S}$$

Since conformal transformations preserve both A_z and $\boldsymbol{H}\cdot d\boldsymbol{l}$, we may choose to perform this integral in u-space, which results in a much simpler calculation.

Since E is given by:

$$E = j\omega\sum_{\substack{k=0\\ k\ \text{even}}}^{N} A_k\cos k\tau \tag{18}$$

and, from (16):

$$H\tau = \frac{I}{2\pi} - \frac{1}{\mu_0}\sum_{\substack{k=2\\ k\ \text{even}}}^{N} kA_k\cos k\tau \tag{19}$$

the losses per unit length are given by

$$\text{losses} = \Re\left\{\int_0^{2\pi}\left(j\omega\sum_{\substack{k=0\\ k\ \text{even}}}^{N} A_k\cos k\tau\right) \times \left(\frac{\bar{I}}{2\pi} - \frac{1}{\mu_0}\sum_{\substack{k=2\\ k\ \text{even}}}^{N} k\bar{A}_k\cos k\tau\right)d\tau\right\}$$

Averaging with respect to time has been performed in the standard way; i.e. by multiplying $\boldsymbol{E}$ by the conjugate of $\boldsymbol{H}$ and extracting the real part of the product.

Note that, when $k \neq l$:

$$\int_0^{2\pi}\cos(k\tau)\cos(l\tau)d\tau = 0$$

Hence, the product of two sums may be reduced to a single sum of products, and we obtain:

$$\text{losses} = \Re\left\{j\omega\int_0^{2\pi}\left(\frac{I}{2\pi}A_0 + \frac{1}{\mu_0}\sum_{\substack{k=2\\ k\ \text{even}}}^{N} k\bar{A}_k A_k\cos^2 k\tau\right)d\tau\right\}$$

Finally, since $\Re(j\omega\bar{A}_k A_k) = 0$ only the first term remains.

The resistance per unit length is therefore given by:

$$R = \Re(j\omega A_0/I)$$

The dimensionless graph in Fig. 8 has been obtained using the above method. This graph may be used to estimate the AC resistance of any rectangular conductor for which $b < a$ and $\Delta > b$.

An estimate of the low-frequency inductance may be obtained from

$$\frac{\mu_0}{2\pi}\ln\left(\frac{R_{\text{return}}}{a/2}\right) + \Re\left(\frac{A_0}{I}\right)$$

This is a high estimate since the current has been concentrated on the major axis of the conductor. The associated errors may be large if the assumption $b \ll a$ is not satisfied.

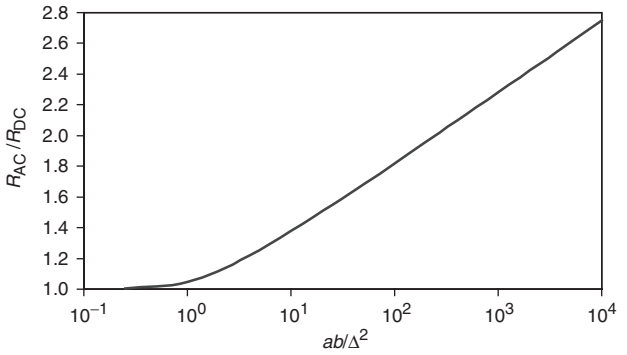

Fig. 8 *Dimensionless graph of R_{AC}/R_{DC} for the low-frequency model*

10 Comparison of resistance calculations for a rectangular strip

Figure 9 shows the resistance per unit length multiplied by the quantity $\sigma\Delta a$ plotted against the ratio b/a. The graph compares the semi-analytical results obtained using (12) with results obtained using values of $H_{surf}^2 dl$ from finite element models. These finite element models use a boundary condition to represent the surface of the conductor; hence, all these models ignore flux penetrating the conductor.

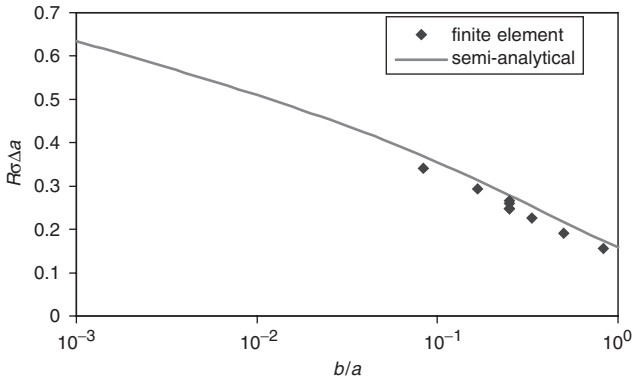

Fig. 9 *$R\sigma\Delta a$ plotted against the ratio b/a*

There are large discrepancies between the results obtained from the finite element models and those obtained using conformal transformations. It is believed that these discrepancies are due to the difficulty experienced by the finite element package in modelling the infinity in $\boldsymbol{H}$ that occurs at each corner of the strip. This hypothesis is supported by the results in Fig. 10, which show that the error can be reduced by the use of much lower mesh error tolerances. The presence of a singularity on the integration path requires a much finer mesh than would be suggested by the mesh error estimates.

Separate finite element models were built to test the accuracy of the resistance estimates produced by the methods described in Sections 7 and 9. These finite element models include the conductor and represent the case when the skin depth is finite. Suitable values of frequency were chosen in order to vary the ratio of skin depth to thickness.

The ratio of the resistance calculated by the finite element model to that obtained using conformal mapping theory is plotted in Fig. 11 as a function of the ratio Δ/b. The high-frequency conformal transformation model was found to give reasonable estimates of the resistance, for all cases where $\Delta < b$.

Figure 12 shows the ratio of the resistance estimates obtained from the finite element package and the low-frequency model. Good agreement is obtained for large values of Δ/b.

It may be noted that the limit of validity, for both methods, occurs at $\Delta \approx b$. Hence, it is possible to obtain a reasonable estimate of resistance for any Δ/b using the appropriate method.

Figure 13 compares the resistance calculated using the finite element model, with the estimates obtained from the two semi-analytical methods. The higher of the two approximations is assumed to give the better estimate of the resistance. For the thin strip considered, this estimate is always within 10% of the finite element result.

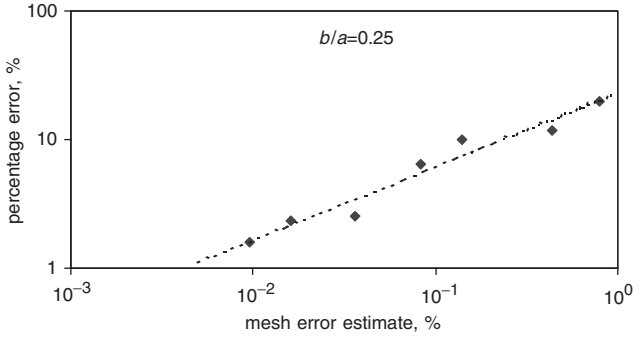

Fig. 10 *Percentage error in $H_{surf}^2 dl$ as a function of the mesh error estimate*

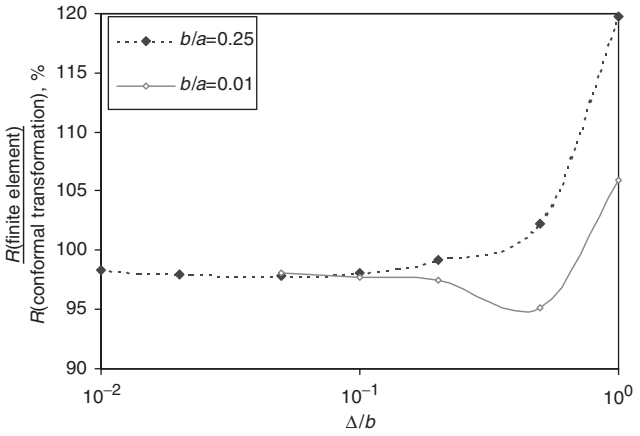

Fig. 11 *The ratio of the numerical and analytical results as a function of Δ/b in the high-frequency regime*

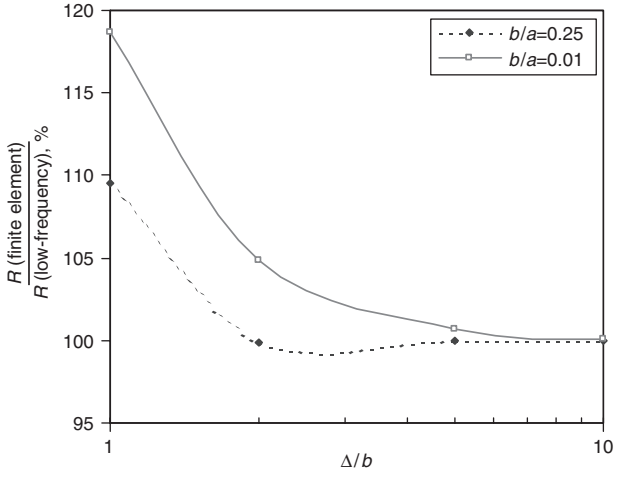

Fig. 12 *The ratio of the numerical and analytical results as a function of Δ/b in the low-frequency regime*

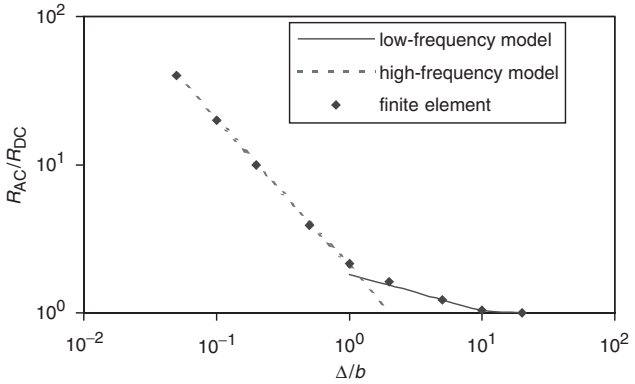

Fig. 13 *Comparison of resistance calculations for a thin strip ($b/a = 0.01$)*

11 Conclusions

For regular n-sided polygons, a semi-analytical method has been obtained to compute the high-frequency AC inductance. For comparison, the DC inductance was calculated using finite element analysis. A method is described which allows the infinite boundary to be modelled without the need to extend the model to large radii. Although no estimates are made of the resistance, the high-frequency resistance of a polygon may be calculated using the same technique as that applied to the rectangular conductors.

For rectangular conductors, the high-frequency and low-frequency AC resistance can be obtained using semi-analytical methods without requiring finite element software. Moreover, the results of these calculations can be described by the pair of dimensionless graphs in Figs. 7 and 8. Using these two methods, the resistance can usually be estimated to within 10%.

12 References

1 Grover, F.W.: 'Inductance calculations, working formulas and tables', (Dover, New York, 1962)
2 Gibbs, W.J.: 'Conformal transformations in electrical engineering', (Chapman & Hall, London, 1958)
3 Abramovitz, M., and Stegun, I.A.: 'Handbook of mathematical functions', (Dover, New York, 1965)